

# COMPARISON OF SIMULATED SEISMIC WAVE WITH SEISMIC WAVE CHARACTERISTICS FOR DESIGN USING GENERAL-USE FAULT MODEL

Takahisa ENOMOTO\* and Takahiro KUNII\*\*

The following are some approaches in the study on the seismic wave characteristics for the earthquake resisting design. The seismic wave characteristics are in general explained by the statistical method using various records of strong earthquake wave and are expressed in the attenuation formula of the max. acceleration and also in the response spectrum. In this paper, we utilized the fault models modified from Haskell model and the specific barrier model for the magnitude (M) of earthquake on a scale of 6-8 and then we examined the seismic wave characteristics. Finally we have made comparison between the above results and those stipulated by the Specifications for Earthquake Resisting Design of Highway Bridges.

*Keywords* : Input seismic wave, response spectra, attenuation curve, fault model

## 1. INTRODUCTION

The calculation of maximum acceleration response spectrum of the seismic wave used for the earthquake resisting design of structures in civil engineering is often based on the regression curve obtained from a large number of record of strong earthquakes as shown in the Specifications for Earthquake Resisting Design of Highway Bridges (SERDHB)<sup>1)</sup>. This regression curve is drawn up, taking as parameters the magnitude and the epicentral distance which are measured for the respective ground conditions. However, it is found that seismic waves have different characteristics even at the same measuring point using the same parameters<sup>2),3)</sup> and also the survey results indicate that structures located in the area along the fault plane near the seismic fault which is regarded as the seismic source in the event of a short-range earthquake, are likely to be hit most seriously<sup>4),5)</sup>.

It is believed to be useful in the design of seismic wave to take into account the effect of the characteristics of seismic source and of the propagating process for the reason that the past record shows the earthquake is often a short-range and large scale one.

Now a study is under way to explain the damage distribution by applying the fault seismic source model and to examined the simulation using response spectrum<sup>6)-8)</sup>.

In some cases, the time series wave-form of input

seismic wave is necessary in the dynamic analysis. However, under the earthquake resisting design method of today the simulated seismic wave obtained either by the seismic motion statistically predicted from the records of a large number of actually observed earthquakes and data of by the average response spectrum<sup>4)-12)</sup> is also often utilized as a highly effective method.

However, no detailed examination has been made to observe how much the difference will be between the above methods and the one where the seismic motion characteristics are evaluated under the same conditions using the fault model with respect to the source mechanism available in practice at this moment.

Therefore, in this regard, it will be very interesting to study this subject. The authors have been studying the simulation method of seismic waves using the macroscopic fault model and the characteristics of amplitude and have obtained comparatively satisfactory results on this method<sup>13)</sup>.

This paper is aimed at making a comparative study of the characteristics of seismic waves (relationship between the max. acceleration and the epicenter distance, and the acceleration response spectrum curve) stipulated by SERDHB widely used now as the quake-resisting design method. It is also aimed at conducting a fundamental review of the technological evaluation procedure of the calculation results by using the fault model which has been generally used as simplified model, with attention paid to the difference of the characteristics of seismic waves due to the variation of the characteristics of source.

Study has been widely under way both from the theoretical and practical viewpoints regarding individual earthquakes in an attempt to uncover

\* Member of JSCE, M. Eng., Kanagawa University, Research Associate (3-27-1 Rokkakubashi Kanagawa-ku Yokohama-shi 221)

\*\* Member of JSCE, Dr. Eng., Tokyo Metropolitan University, Professor

the minute details of the fracture phenomenon spread over the fault with the progress of the earthquake<sup>14)~18)</sup>. However, in this paper, the comparison is made between the average characteristics of seismic wave obtained from the fault model, which is readily available from the technological viewpoint, and those for the design of seismic wave. Two types of model are used as a fault model: the Haskell model<sup>19),20)</sup> and the Specific Barrier model<sup>21)</sup>. The former is a typical macroscopic fault model and has a relatively explicit calculation method, while the latter is a microscopic fault model made with respect to the lack of uniformity.

## 2. FAULT MODEL

### (1) Macroscopic fault model

The Haskell model is assumed to be a rectangular fault measuring in length  $L$  and width  $W$ , situated in an infinite space medium comprised of a uniform elastic body, in order to express the full detail of the structure of the fault in a simplified form as shown in Fig.1, while the movement (fracture) of fault is assumed to be propagated along the longitudinal direction from the end of the fault and the velocity of fracture propagation to be constant. It is found that dislocation occurs at an arbitrary point on the fault at the same time as the fracture front arrives, and such dislocation stops after a certain time  $\tau$  elapses (rise time), leaving the permanent displacement  $D$  (final dislocation amount). In this case,  $\tau$  and  $D$  are assumed to be equal at any point on the fault, and the time function (source time function) to be expressed in the ramp function as indicated in Fig.2 (a). The Haskell model is a macroscopic model to evaluate the fault movement and also the seismic wave generated therefrom. The spectrum of the seismic motion at the ground surface is to be calculated by multiplying the incident seismic wave spectrum which comes into the seismic basement multiplying by the transfer function between the basement and the ground surface. If the transfer function is  $H(\omega)$ ,

$$|\ddot{U}(\omega)| = \mu \cdot LWD \cdot R(\theta, \phi, r) \cdot \{G(\omega) \omega^2\} \cdot \{F(\omega, \tau_0) \cdot \omega\} \cdot Q(\omega) \cdot H(\omega) \quad (1)$$

- Where,  $\omega$ : Circular frequency  
 $\mu$ : Rigidity of medium  
 $R(\theta, \phi, r)$ : Radiation of body wave  
 $G(\omega)$ : Fourier transform of dislocation time function  
 $F(\omega, \tau_0)$ : Function to express the effect of moving source  
 $Q(\omega)$ : Function to express the damping effect

The acceleration Fourier spectrum at the

measuring point will be determined by the above formula.

### (2) Microscopic fault model

In the case of macroscopic fault model, the short period component tends to be undervalued for the reason that the heterogeneity on the fault is not considered. In order to compensate for this, a special method is to be applied, such as providing fluctuation to the time function of dislocation, but the Specific Barrier model proposed by Dr. K. Aki *et al.* has been used recently as a fault model directly taking into account the heterogeneity effect on the fault (Fig.3). This model is based on the assumption that the fault is an assembly of small elements (small circular cracks), the clearance of circular cracks is regarded as a barrier and the fracture of circular cracks propagates gradually on the fault. On this model, the Fourier spectrum of a strong seismic wave generated by the entire part of the fault can be evaluated by superimposing the acceleration Fourier spectrums of the seismic wave generated by the circular cracks, which can be calculated by the theoretical solution advocated by Dr. Sato and Hirasawa<sup>23)</sup>. In this paper, the acceleration Fourier spectrum generated by the individual circular cracks is to be calculated by the above method and to be superimposed with the element acceleration wave in the time domain after being subjected to Fourier inverse conversion to create the compound wave. After being subjected to Fourier conversion again, the acceleration Fourier spectrum of the aforesaid compound wave is to be obtained. If the damping parameter of distance is  $Q(\omega)$  and the transfer function between the seismic basement and the observation site is  $H(\omega)$ ,

$$|\ddot{U}(\omega)| = \{F_s / (4\pi\beta r)\} A(\omega) Q(\omega) H(\omega) \quad (2)$$

- Where,  $F_s$ : Radiation of double couple point source  
 $\beta$ : S wave velocity of medium  
 $r$ : Hypocentral distance  
 $A(\omega)$ : Acceleration Fourier spectrum of circular crack

In this study, the acceleration Fourier spectrum of the seismic wave generated from one circular crack is calculated by the above method. Phase parameters are required in the case of Fourier inverse conversion into the time domain and uniform random numbers are entered in this paper.

## 3. SETTING OF ANALYTICAL CONDITIONS

### (1) Seismic fault parameter

- a) Fault model parameters of Haskell model

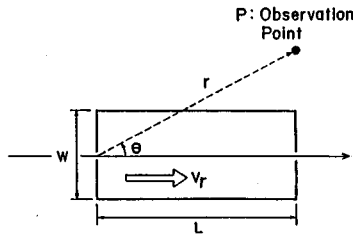


Fig.1 General conception of Haskell Model.

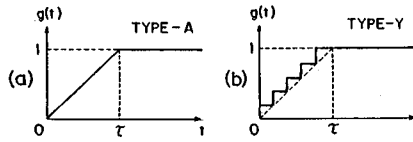


Fig.2 Source time function of Haskell Model.

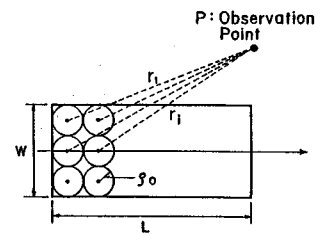


Fig.3 General conception of Specific Barrier Model.

Table 1 List of fault parameters.

	Haskell Model			Specific Barrier Model		
	M=6	M=7	M=8	M=6	M=7	M=8
Radius of Crack (rho) km	-	-	-	0.99	4.38	11.2
Number of Crack (n)	-	-	-	21(7x3)	15(5x3)	18(6x3)
Fault Length(L) km	16.0	50.0	160.0	13.9	43.8	134.0
Fault Width(w) km	8.0	25.0	80.0	5.9	26.3	67.0
Area of Fault Plane (A) km <sup>2</sup>	128	1250	12800	82	1152	8978
Dislocation (D) cm	52.5	166.0	525.0	52.5	166.0	525.0
Wave Velocity (beta) km/s	3.0	3.0	9.0	3.0	3.0	3.0
Rigidity (mu) dyn cm	2.7x10 <sup>11</sup>	2.7x10 <sup>11</sup>	2.7x10 <sup>11</sup>	2.7x10 <sup>11</sup>	2.7x10 <sup>11</sup>	2.7x10 <sup>11</sup>
Stress Drop (delta sigma) bar	16.9	17.1	16.9	131.1	93.7	116.2
Rupture Velocity (Vr) km	2.16	2.16	2.16	2.16	2.16	2.16
Rise Time (tau) s	2.31	7.20	23.1	-	-	-
Damping Factor (Q)	250	250	250	250	250	250

It is necessary to determine the various fault model parameters for calculation of the acceleration Fourier spectrum of seismic wave predicted from Haskell model. In the case of typical earthquakes the fault model can be obtained from literature<sup>24)</sup> and also ones in Japan can be projected from various observation data<sup>25)</sup>. In this paper, fault model parameters, which are mainly determined by taking magnitude (M) as a variable, are established in the following manner :

- 1) Length of fault (L)<sup>26)</sup>, width<sup>27)</sup>  
 $\log D = 0.5M - 1.8, W = L/2$  (km)
- 2) Max. dislocation (D)<sup>28)</sup>  
 $\log D = 0.5M - 1.28$  (cm)
- 3) Modulus of rigidity (mu)  
 $\mu = \rho\beta^2, \rho$ : density of medium
- 4) Stress drop (delta sigma)<sup>29)</sup>  
 $\Delta\sigma = k\mu D\sqrt{A}, k = (4L)/(\pi\sqrt{W}) = 1.80$
- 5) Velocity of fracture propagation  
 $V_r = 0.72\beta$  (km/s)
- 6) Rise time (tau)<sup>30)</sup>  
 $\log(2\pi\tau) = 0.5M - 2.42$  (s)
- 7) Damping coefficient (Q)<sup>31)</sup>  
 $Q = 100(\beta - 0.49)$

Parameters established are shown in Table 1.

Since the Haskell model in general utilizes ramp function as the source time function, such a model can hardly explain a short period seismic wave which lasts for less than a few seconds but poses significant meaning from the viewpoint of seismology. From the above viewpoint, an effort is made in this paper to evaluated the short period component by providing fluctuation to the time

function of dislocation. Among various assumptions by the authors, source time function with stepwise fluctuation is used. The following show the source time function (Fig.2 (b)) and Fourier conversion form. In this paper, the number of fluctuation n is estimated to 5.

8) Source time function (g(t))<sup>32)</sup>

$$g(t) = \begin{cases} 0, & t < 0 \\ \frac{1}{n+1}, & 0 \leq t < \frac{\tau}{n} \\ \frac{2}{n+1}, & \frac{\tau}{n} \leq t < \frac{2\tau}{n} \\ \frac{3}{n+1}, & \frac{2\tau}{n} \leq t < \frac{3\tau}{n} \\ \vdots & \vdots \\ \frac{n}{n+1}, & \frac{(n-1)\tau}{n} \leq t < \tau \\ 1, & \tau \leq t \end{cases} \dots\dots\dots (3)$$

The Fourier conversion (G(omega)) of source time function will be

$$G(\omega) = \{Rn(\omega)^2 + In(\omega)^2\}^{1/2} \dots\dots\dots (4)$$

$$Rn(\omega) = [(1+n)\omega]^{-1} \{-\sin(\omega\tau/n) - \sin(2\omega\tau/n) - \sin(3\omega\tau/n) - \sin(4\omega\tau/n) - \dots\dots\dots - \sin((n-1)\omega\tau/n) - \sin(\omega\tau)\} \dots\dots\dots (5)$$

$$In(\omega) = [(1+n)\omega]^{-1} \{-1 - \cos(\omega\tau/n) - \cos(2\omega\tau/n) - \cos(3\omega\tau/n) - \cos(4\omega\tau/n) - \dots\dots\dots\} \dots\dots\dots (6)$$

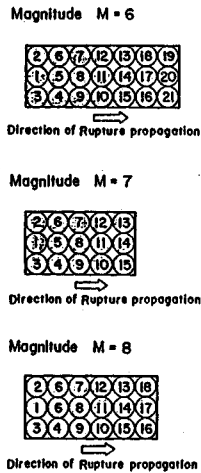


Fig. 4 Setting of circular cracks and fracture propagation procedure for Specific Barrier Model (Numeral in figures indicates the order of fracture propagation in this study).

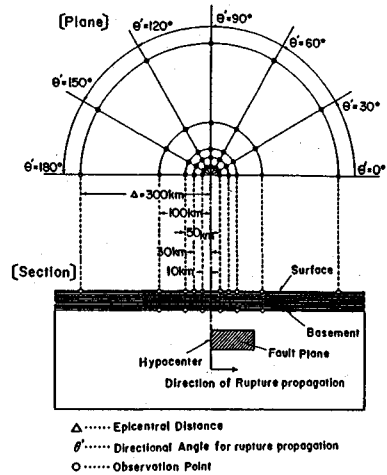


Fig. 5 Setting of calculation points.

$$-\cos((n-1)\omega\tau/n) - \cos(\omega\tau)$$

b) Fault model parameters of Specific Barrier model

It is necessary to set up various fault model parameters in calculation of seismic wave using Specific Barrier model. Fault model parameters of the Specific Barrier model differ from those of the Haskell model in that the fault does not form a large fault plane but an assembly of many small circular cracks, that is, what determines the fault plane in the case of the Specific Barrier model depends on the radius and number of circular cracks. The local stress drop can be also adjusted by setting up the circular crack unit. However, in the case of the fault model parameters other than the above, the same level of parameters is used as for Haskell. Dr. Aki<sup>33)</sup> et al. projected the diameter of circular crack and fault model parameters such as stress drop in various earthquakes.

On the other hand, Dr. Kamiyama<sup>34)</sup> induced the expectation value of the acceleration Fourier spectrum by estimating the average image of spectrum from 228 element record of strong earthquakes in Japan, as well as considering the Specific Barrier model and then calculating the crack (patch) radius thereby. In this study, according to the results of Dr. Kamiyama's study, the parameter of the radius of the circular crack on the fault plane is to be set up for each level of magnitude, while assuming that all local stress drops are the same. Only circular crack radius ( $\rho_0$ ), number ( $n$ ) and local stress drop ( $\Delta\sigma$ ) are discussed here whereas dislocation ( $D$ ), rigidity of medium ( $\mu$ ) and velocity of fracture propagation ( $V_r$ ) basically use the same parameters as for the

Haskell model.

- 1) Circular crack radius ( $\rho_0$ ), number ( $n$ )<sup>34)</sup>  
 $M=6$ ;  $\rho_0=.99(\text{km})$ ,  $n=21$  [crosswise 7 (pcs),  
lengthwise 3 (pcs)]  
 $M=7$ ;  $\rho_0=4.38(\text{km})$ ,  $n=15$  [crosswise 5 (pcs),  
lengthwise 3 (pcs)]  
 $M=8$ ;  $\rho_0=11.2(\text{km})$ ,  $n=18$  [crosswise 6 (pcs),  
lengthwise 3 (pcs)]
- 2) Local stress drop ( $\Delta\sigma$ )<sup>21)</sup>  

$$\frac{D}{\rho_0} = \frac{24}{7\pi} \cdot \frac{\Delta\sigma}{\mu}$$

Parameters determined are shown in Table 1. The sequence of fracture propagation of circular crack is shown in Fig. 4, wherein the expansion of fracture front on the fault plane is assumed to begin at an arbitrary point and to propagate toward the arbitrary direction.

(2) Location of measuring points

The spectrum of body wave estimated from the fault model is subject to change by the locational relationship between the fault plane and the measuring point, i.e., the distance from the epicenter to the measuring point and the direction ( $\theta^\circ$ ) of the measuring point with regard to the direction of fracture propagation of fault. It is known that the characteristics of seismic wave in the actual earthquake are affected by the epicentral distance and the measuring direction with regard to the fracture propagation direction.

In this paper, 7 directions,  $\theta^\circ=0^\circ, 30^\circ, 60^\circ, 90^\circ, 120^\circ, 150^\circ$  and  $180^\circ$ , relative to the direction of fracture propagation of fault, are analyzed in a study of the influence of direction. It is also acknowledged that there is difference in the

	H(m)	$\beta$ (m/s)	$\rho$ g/cm <sup>3</sup>	Q
1	20	250	1.7	20
2	300	550	1.9	50
3	430	670	2.0	50
4	1820	1500	2.2	100
5	--	3000	2.5	250

Fig.6 Underground condition.

characteristics of seismic waves even in the same direction if the epicentral distance is different. In this paper, 5 epicentral distances,  $\Delta=10$  km, 30 km, 50 km, 100 km and 300 km, are taken up to study the above. The location of measuring points are charted in Fig.5. In this paper, the depth of hypocenter is estimated to 30 km.

(3) **Underground model**

It is necessary to determine the ground structure and to make a model in order to calculate simulated seismic wave of the ground and to make comparison with the seismic wave for design. Study is now vigorously under way concerning the structure of ground at the deep level, particularly in the Kanto area, and the basement and the structure of ground are gradually disclosed<sup>22)</sup>. In this paper, while respecting the structure of ground around Tokyo, we have supposed the ground model with the horizontal boundary on the half space elastic medium, which presumes the seismic basement with parameters shown in Fig.6. On the other hand, according to the classification of ground condition stipulated by SERDHB, the ground model proposed here is equivalent to the second class of ground condition. The calculation results of the transfer function of the ground model introduced here using the multi-reflection are shown in Fig.7.

4. **RELATIONSHIP BETWEEN THE MAX. ACCELERATION AND EPICENTRAL DISTANCE**

(1) **Relationship based on SERDHB**

The SERDHB provides various regression curves depicting the relationship between the max. acceleration and the epicentral distance according to the classification of ground conditions. The classification of ground conditions used for analysis comprises 4 kinds from class 1 to 4. The ground model assumed here falls in class 2 category.

In the SERDHB, regression curve is obtained through the multi-regression analysis by assuming the seismic wave characteristics parameter ( $\alpha$ ) with regression curve formulas (7).

$$\alpha = a \cdot 10^{bM} \cdot (\Delta + \Delta_0)^c \dots\dots\dots (7)$$

$\alpha$ : seismic wave characteristic parameter,

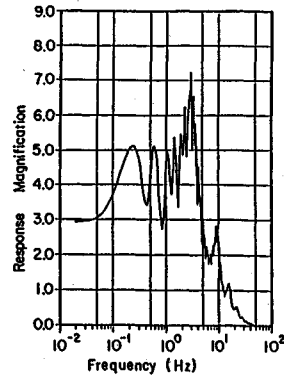


Fig.7 Transfer function of underground structure model (From seismic basement to ground surface).

maximum horizontal acceleration  $A_{max}$  (gal)

$a, b, c$ : constant,  $M$ : magnitude of earthquake,  $\Delta$ : epicentral distance (km),  $\Delta_0$ : constant (= 10 km)

(2) **Calculation result by fault model**

The acceleration time series waveform is calculated using two fault models in the time domain by various parameters set up in Table 1, and then the correlation between the max. value and the epicentral distance of measuring point is studied. As mentioned earlier, it is learnt from the calculation result with the fault model that the characteristics of seismic wave are varied even with the same epicentral distance if the relative position of the measuring point toward the direction of fracture propagation on the fault is different. In this paper, the max. acceleration is calculated in each case where  $\theta'$  is 0°, 30°, 60°, 90°, 120°, 150° and 180° and the variation range by the direction is charted in Fig.8 (a) to (f).

The locational relationship of the measuring point relative to the direction of fracture propagation is not reflected on the regression curve concerning the relationship between the max. acceleration and epicentral distance by the SERDHB. For this reason, it is appropriate to take the average value of the max. acceleration calculated on the fault model in each direction in order to compare with the result of calculation by the regression curve obtained by the SERDHB. Therefore, the average values are plotted and linked with bold line as shown in Fig.8 (a) to (f) and compared with those of the SERDHB (drawn in broken line).

The max. value of the seismic wave at each measuring point on the ground surface, which is calculated by the Haskell model, is charted in Fig.8 (a), (b), (c) and that calculated by the Specific

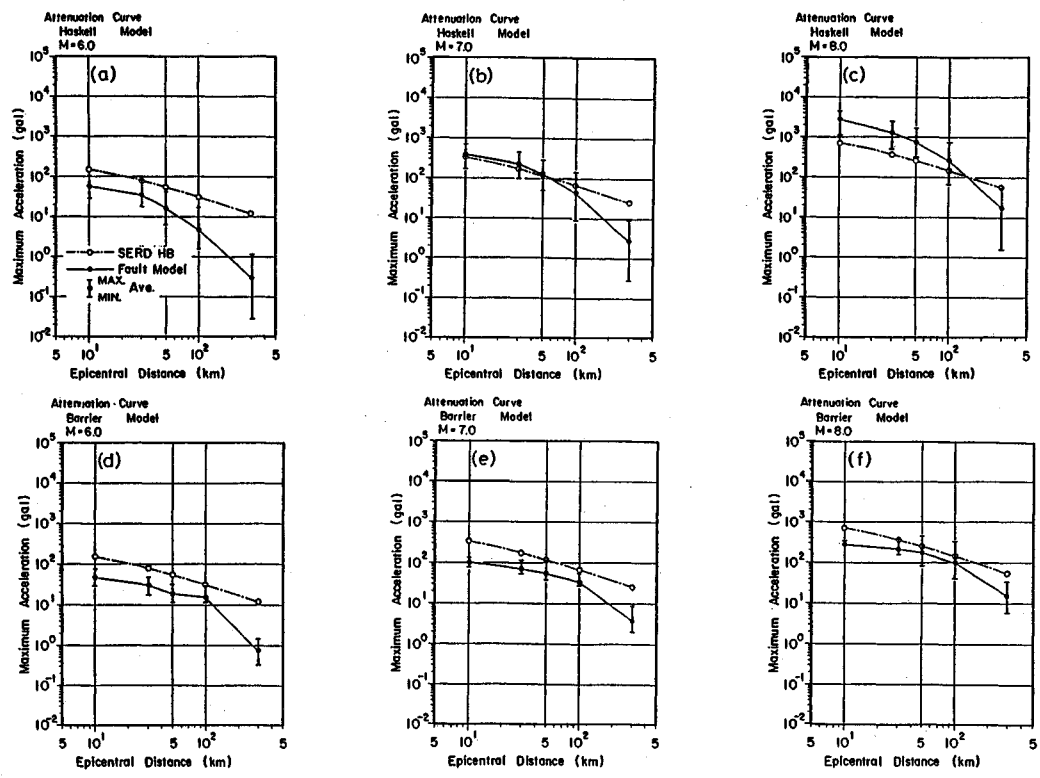


Fig.8 Comparison with the relation between maximum acceleration value and epicentral distance by SERDHB.

Barrier model in Fig.8 (d), (e) and (f), classified by the epicentral distance and the direction.

(3) Comparative study

In comparison with the results obtained by the SERDHB, those on the Haskell model, where  $\Delta = 10-100$  km, show lower value in the case of  $M=6$  and conversely slightly higher one in the case of  $M=8$ , whereas they become similar in the case of  $M=7$ . Where  $\Delta = 300$  km, all the cases in  $M=6-8$  show lower values. On the other hand, those on the Specific Barrier model are lower than those obtained by the SERDHB. This suggests that setting of parameters on both models needs to be partially revised but in this paper, this must be also attributed to the effect of change (non-linearization) of the stiffness and damping capability corresponding to the strain level on the surface ground due to the possible influence of the surface wave component which has not been considered in this paper. As far as the variation by the measuring point direction relative to the direction of fracture propagation of the fault is concerned, the calculation results on the Haskell model are apt to present larger variation than the Specific Barrier model.

5. ACCELERATION RESPONSE SPECTRUM CURVE

(1) Acceleration response spectrum curve by the SERDHB

The SERDHB provides the acceleration response spectrum through the analysis of earthquake, record of 227 elements from 68 earthquakes measured on the ground in Japan.

Following Housner's definition, the absolute acceleration response spectrum is expressed by  $S_A$ .

The magnitude of the seismic wave acceleration does not directly affect the response spectrum and as the spectrum value can be the average value among many response spectrums, non-dimensional response spectrum of the response spectrum magnification  $\beta$  defined in formula (8) is used.

$$\beta = \frac{S_A}{Z_{max}} \dots \dots \dots (8)$$

$Z_{max}$ : Max. acceleration of seismic motion

The calculation results of response spectrum magnification (damping constant  $h=0.05$ ) on two fault models as per the SERDHB are shown in Fig.9 and Fig.10 with broken line in the following cases, where  $M=6$  (corresponding to the case

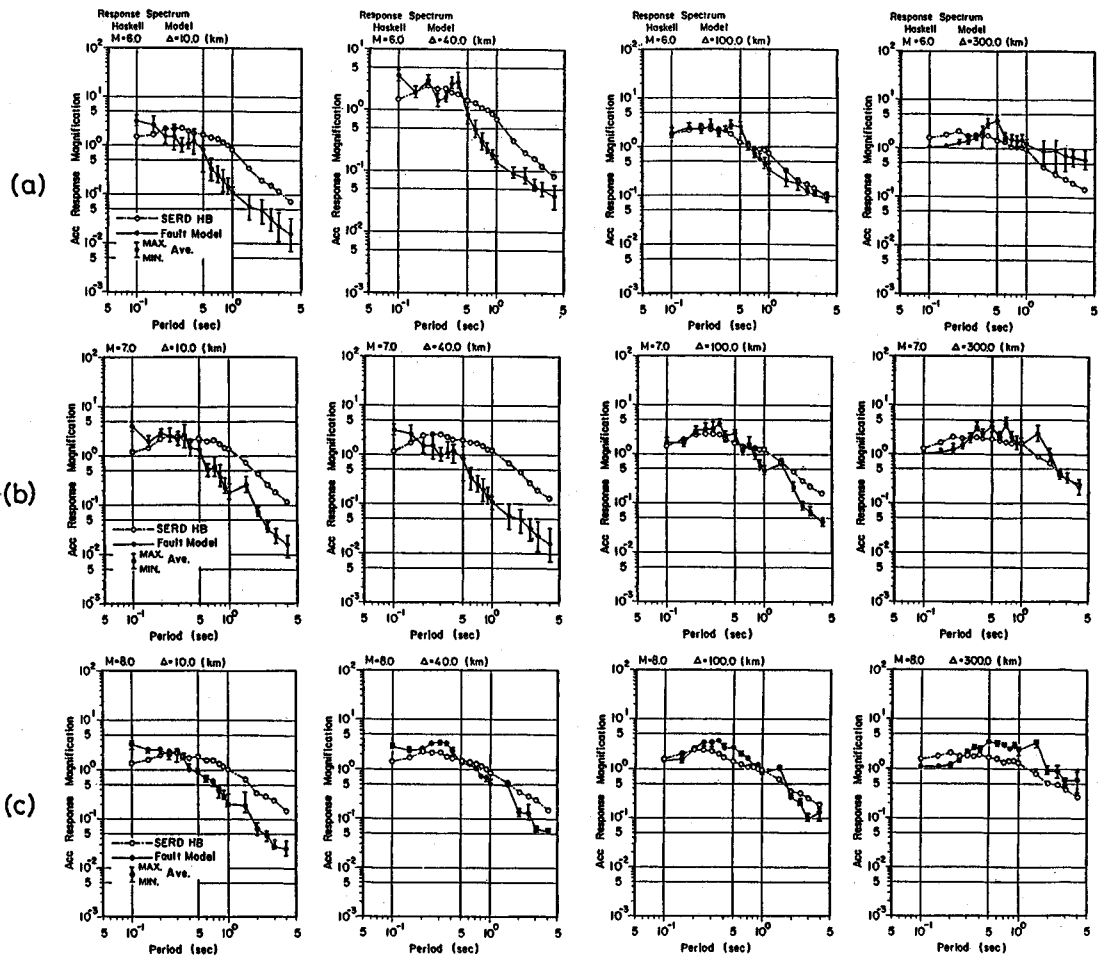


Fig.9 Comparison with the acceleration response spectra by SERDHB (Case of Haskell Model).

when  $M=5.4-M=6.0$ , 7 (corresponding to the case where  $M=6.8-M=7.4$ ), 8 (corresponding to the case where  $M=7.5-M=7.9$ ),  $\Delta$ =epicentral distance 10 km (corresponding to the case of less than 20 km), 40 km (the average value of calculation to 20-59 km), 100 km (corresponding to 60-119 km) and 300 km (corresponding to 200-405 km).

(2) Acceleration spectrum curve by fault model

The response spectrum magnification ( $\beta$ ) is obtained in formula (8) each for the acceleration waveform of the simulated seismic wave measured in the same manner as for the previous clause at each measuring point on the ground surface, and then the acceleration response spectrum magnification curve (damping constant  $h=0.05$ ) is computed. These are based on the calculation results under the ground condition of class 2. The variation range of the response spectrum magni-

fication by the direction ( $\theta'$ ) relative to the direction of fracture propagation of fault model is charted in Fig.9 to Fig.10 and the average values are linked with bold line.

(3) Comparative study

Calculation results on the Haskell model, classified by  $M$  and  $\Delta$  are shown in Fig.9 (a) to (c) in contrast with Fig.10 (a) to (c) showing those of the Specific Barrier model.

Where  $M$  is 6 (Fig.9 (a), Fig.10 (a)), the Haskell model shows almost similar values in case of  $\Delta=100$  km. When  $\Delta$  is shorter than the above, the response spectrum magnification becomes smaller in the long period domain whereas when  $\Delta$  is longer, it is larger. On the other hand, the Specific Barrier model shows comparatively similar values in the case of  $\Delta=40$  km and 100 km. When  $\Delta$  is shorter, the magnification becomes smaller in the long period domain in the case of  $\Delta=10$  km and in the longer case  $\Delta=300$  km (Fig.10 (a)), it becomes

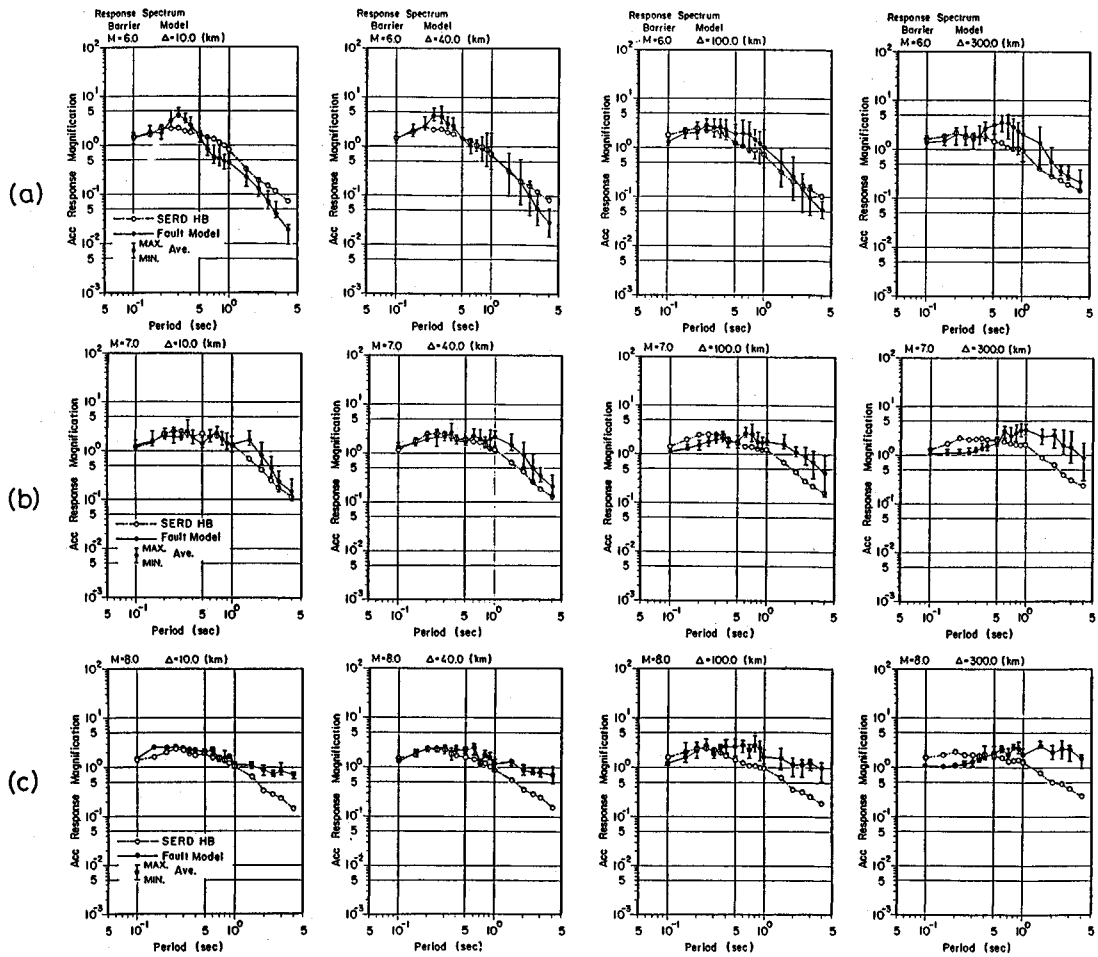


Fig.10 Comparison with the acceleration response spectra by SERDHB (Case of Specific Barrier Model).

larger in the same domain.

Where  $M$  is 7 (Fig.9 (b) and Fig.10 (b)), the Haskell model shows almost similar values in the case of  $\Delta=300$  km (Fig.9 (b)), the shorter  $\Delta$  is, the smaller the response spectrum magnification becomes in the long period domain. Conversely, the Specific Barrier model shows comparatively similar values in the case of  $\Delta=10$  km, the longer  $\Delta$  is, the larger the magnification in the long period domain.

Where  $M$  is 8 (Fig.9 (c), Fig.10 (c)), the Haskell model shows comparatively similar values in the case of  $\Delta=40$  km, 100 km. When it is shorter, the magnification becomes smaller in the long period domain whereas in the longer case, it becomes larger. On the other hand, the Specific Barrier model shows larger values in the same domain in both cases. As a whole, it shows larger values in the long period domain. When  $M$  is 7 and  $\Delta$  is 100 km, the calculation results on the fault model become

comparatively similar to those of the SERDHB.

It is revealed from the results that the Haskell model tends to show larger values in the long period domain when the epicentral distance is long. The variation by the direction is larger in the case of the Specific Barrier model.

## 6. CONCLUSIONS

The following summarize the analytical results of this paper.

(1) Comparison was made between the seismic wave characteristics in the case using the fault model and those for design as regard the relationship between the max. acceleration and the epicentral distance. As a result, it is found that the Haskell model shows comparatively similar values in a range  $\Delta=10$  km to 100 km when  $M$  is 7, but smaller values at  $\Delta=300$  km in all cases when  $M=6$  to 8. On the other hand, the Specific Barrier model shows smaller values in all cases. In this regard, it is



necessary to amass research and study to allow parameter for the model under this method. As regards the fact that the magnification tends to be lower as the epicentral distance becomes larger, it is necessary to consider the effect of the surface wave component.

(2) In order to study the characteristics of period of seismic wave calculated here, the acceleration response spectrum magnification curves are calculated and compared. Consequently, it is noted that there is a conspicuous difference between both fault models, that is, the Haskell model tends to show smaller values in the long period domain when the epicentral distance is short but the Specific Barrier model larger values in the same domain in the longer distance. The variation by the direction is likely to be larger in the case of the Specific Barrier model and the variation of the characteristics of seismic wave is greatly affected by the direction.

**Acknowledgement:** We would like to express our sincere gratitude to Mr. Masuji Yasuda in Kajima Construction Co., Ltd. (formerly of the graduate school of Tokyo Metropolitan University) for his cooperation. Our gratitude also goes to Professor Morihisa Fujimoto in Dept. of Architecture, Faculty of Engineering, Kanagawa University, who has rendered us incessant encouragement and assistance.

#### REFERENCES

- 1) Road Association of Japan: Specification of Highway Bridges and It's Explanations. V Earthquake Resistant Design, May, 1985.
- 2) Mochizuki, T. and Enomoto, T.: On Earthquake Wave Characteristics in Kanto District Considering Source and Underground Condition. The 21 th Symp. on Natu. Disas. Sci., pp.133-136, Dec., 1984.
- 3) Kinoshita, S.: Spectral Characteristics of Bedrock Motion in the Tokyo Metropolitan Area, Proc. of JSCE, No.344/ I-1, pp.89-94, April, 1984.
- 4) Earthquake Research Group of Tokyo Metropolitan University: Research Report on Recent Directly Under Type Earthquakes, August, 1976.
- 5) Miyatake, T.: Earthquake Source Process and Damage Distribution, ZISIN, Jour. of the Seismol. Soci. of Japan, Vol.37, No.2, pp.257-267, June, 1984.
- 6) Inoue, R.: Studies on Design Earthquake in The Period Range of 2 to 20 sec. A Review, Proc. of JSCE, No.374/ I-6, pp.1-23, Dec., 1986.
- 7) Inoue, R., Fujino, Y., Matsubara, K. and Hakuno, M.: Estimation of Relatively Long-Period Ground Motions by a Fault Dislocation Theory, Proc. of JSCE, Vol.317, pp.47-60, Janu., 1982.
- 8) Takemura, M. and Ikeura, T.: Semi-Empirical Synthesis of strong Ground Motion for the Description of Inhomogeneous Faulting, ZISIN, Jour. of the seismol. Soci. of Japan, Vol.40, No.1, pp.77-88, March, 1987.
- 9) Katayama, T., Iwasaki, T. and Saeki, V.: Statistical Analysis of Earthquake Acceleration Response Spectra, Proc. of JSCE, Vol.275, pp.19-40, July, 1978.
- 10) Goto, H., Kameda, H. and Sugito, M.: Prediction of Strong Earthquake Motions by Evolutionary Process Model, Proc. of JSCE, Vol.286, pp.37-51, June, 1979.
- 11) Kawashima, K. and Aizawa, K.: Attenuation of Earthquake Response Spectra Based on Multiple Regression Analysis of Japanese Strong Motion Data, Proc. of JSCE, Vol.350/ I-2, pp.181-186, Dec., 1984.
- 12) Toki, K., Sato, T. and Kiyono, J.: Synthesizing Design Ground Motions from Microearthquake Records, Proc. of JSCE Structural Eng./Earthquake Eng., Vol.2, No.2, pp.177-187, Oct., 1985.
- 13) Yasuda, M., Tateyama, A., Kunii, T. and Enomoto, T.: On Engineering Estimation of Earthquake Wave Characteristics Based on Fault Model, Proc. of the 16 th of JSCE Kanto Block Teach. Res. Symp., pp.36-39, March, 1989.
- 14) Fujino, Y., Yokota, T., Hamazaki, Y. and Inoue, R.: Multiple Event Analysis of 1979 Imperial Valley Earthquake Using Distinct Phases in Near-field Accelerograms, Proc. of JSCE, No.344.
- 15) Iida, M. and Hakuno, M.: The Synthesis of the Acceleration Wave in a Great Earthquake by Small Earthquake Records, Proc. of JSCE, Vol.329, pp.57-68, Janu., 1983.
- 16) Yamada, Y., Noda, S. and Ohwaki, T.: Evaluation of Ground Motions in Near-Source Region During the 1979 Imperial Valley Earthquake, Proc. of JSCE, Vol.344/ I-1, pp.303-312, April, 1984.
- 17) Akao, Y. and Watanabe, M.: Inversion Analysis for Multiple-Event Process of the 1986 North Palm Spring Earthquake Induced from Strong Motion Accelerograms, ZISIN, Jour. of the Seismol. Soci. of Japan, Vol.41, No.2, pp.247-257, June, 1988.
- 18) Kikuchi, M.: Analysis of Multiple Event Sources, ZISIN, Jour. of the Seismol. Soci. of Japan, Vol.41, No.4, pp.619-628, Dec., 1988.
- 19) Haskell, N.A.: Elastic Displacements in the Near-Field of a Propagating Fault, Bull. of the Seismol. Soci. of America, Vol.59, No.2, pp.865-908, April, 1969.
- 20) Savage, J.C.: Relation of Corner Frequency to Fault Dimensions, Jour. of Geophy. Res., Vol.77, No.20, pp.3788-3795, July, 1972.
- 21) Papageorgiou, S.A. and Aki, K.: A Specific Barrier Model for the Quantitative Description of Inhomogeneous Faulting and the Prediction of Strong Ground Motion. I. Description of the Model, Bull. of the Seismol. Soci. of America, Vol.73, No.3, pp.693-722, June, 1983.
- 22) For example, Seo, K.: Investigation of Deep Underground Effects on Earthquake Motions, The 13 th Symp. on Ground Vibrations, pp.27-34, July 1985.
- 23) Sato, T. and Hirasawa, T.: Body Wave Spectra from

- Propagating Shear Cracks, Jour. Phys. Earth., Vol.21, pp.415-432, 1973.
- 24) Geller, R.J.: Scalling Relations for Earthquake Source Parameters and Magnitudes, Bull. of the Seismol. Soci. of America, Vol.66, No.4, pp.1051-1523, 1976.
- 25) Sato, R.: Handbook of Japanese Earthquake Fault Parameter, Kajima Publishing Co., Mar., 1989.
- 26) Otsuka, M.: Earthquake Magnitude and Fault Formation, Jour. Phys. Earth, Vol.12, pp.19-27, 1964.
- 27) Kanamori, H. and Anderson, D.L.: Theoretical Basis of Some Empirical Relation in Seismology, Bull. of the Seismol. Soci. of America, Vol.65, No.4, pp.1073-1095, 1975.
- 28) Iida, K.: Earthquake Energy and Earthquake Fault, Jour. Earth Sci., Nagoya Univ., Vol.7, pp.98-108, 1959.
- 29) Kanamori, H.: Physics of the Earthquake: Earth Science Series 8, Iwanami Publishing Co., Sept., 1982.
- 30) Ohta, Y. and Kagami, H.: Ultimate Values of Period and Amplitude on Seismic Input Motions in Relation to a Large-Scale Structure, Trans. of AIJ, Vol.249, pp.53-60, Dec., 1976.
- 31) Ishida, K.: A Study on the Estimating the Characteristics of the Strong Motion Spectra, Trans. of AIJ, pp.48-58, April, 1982.
- 32) Kunii, T. and Enomoto, T.: Study on the Analytical Method for Earthquake Motions by Using Source Mechanism-Comparison to the Investigation of Overturning Tomb Stones-, Proc. of the 18th JSCE Earthq. Eng. Symp., pp.9-12, July, 1985.
- 33) Papageorgiou, A.S. and Aki, K.: A Specific Barrier Model for the Quantitative Description of Inhomogenous Faulting and the Prediction of Strong Ground Motion. Part II, Applications of the Model, Bull. of the Seismol. Soci. of America, Vol.73, No.4, pp.953-978, August, 1983.
- 34) Kamiyama, M.: Earthquake Source Characteristics Inferred from the Statistically Analyzed Spectra of Strong Motions with Aid to Dynamic Model of Faulting, Proc. of JSCE, No.386/ I -8, pp.175-184, October, 1987.

(Received October 19, 1989)

## 汎用の断層震源モデルによる模擬地震動と 設計用地震動特性の比較

荻本孝久・国井隆弘

土木構造物の設計用地震動としては、道路橋示方書に示された地震動の最大加速度値と応答スペクトルが用いられる場合が多い。本論文は、汎用の断層震源モデルである Haskell モデルと Specific Barrier モデルを用いて  $M=6, 7, 8$  の地震規模を想定して模擬地震動を作成し、上記示方書による最大加速度値の距離減衰式と応答スペクトルについて比較を行った。その結果から断層震源モデルの工学的利用の可能性について基礎的な考察を行ったものである。